

ResDisMapper: An R package for fine-scale mapping of resistance to dispersal

Qian Tang | Tak Fung | Frank E. Rheindt 

Department of Biological Sciences, National University of Singapore, Singapore City, Singapore

Correspondence

Frank E. Rheindt, Department of Biological Sciences, National University of Singapore, Singapore City, Singapore.
Email: dbrsfe@nus.edu.sg

Funding information

Singapore Ministry of Education Tier 1, Grant/Award Number: WBS R-154-000-691-112; Singapore MSRDP, Grant/Award Number: WBS R-154-000-A47-281; James S. McDonnell Foundation, Grant/Award Number: 220020470

Abstract

Management of biological invasions and conservation activity in the fight against habitat fragmentation both require information on how ongoing dispersal of organisms is affected by the environment. However, there are few landscape genetic computer programs that map resistance to dispersal at small spatiotemporal scales. To facilitate such analyses, we present an R package named *ResDisMapper* for the mapping of resistance to dispersal at small spatiotemporal scales, without the need for prior knowledge on environmental features or intensive computation. Based on the concept of isolation by distance (IBD), *ResDisMapper* calculates resistance using deviations of each pair of samples from the general IBD trend (IBD residuals). The IBD residuals are projected onto the studied area, which allows construction and visualization of a fine-scale map of resistance based on spatial accumulation of positive or negative IBD residuals. In this study, we tested *ResDisMapper* with both simulated and empirical data sets and compared its performance with two other popular landscape genetic programs. Overall, we found that *ResDisMapper* can map resistance with relatively high accuracy. The latest version of the package and associated documentation are available on Github (<https://github.com/takfung/ResDisMapper>).

KEYWORDS

biological invasions, conservation genetics, habitat fragmentation, isolation by distance, landscape genetics

1 | INTRODUCTION

Landscape genetics has become a hot topic in the current era of next-generation sequencing (Richardson, Brady, Wang, & Spear, 2016; Storfer, Patton, & Fraik, 2018). Understanding the association between landscape or other geographical features and population genetic patterns is important for revealing the evolutionary history of species (Palsbøll, 1999) as well as informing their management (Dudaniec et al., 2013). Many computer programs have been developed to analyse these associations after the concept of landscape genetics was developed about 15 years ago (Manel & Holderegger, 2013; Manel, Schwartz, Luikart, & Taberlet, 2003; Storfer, Murphy, Spear, Holderegger, & Waits, 2010).

For examining evolutionary histories in particular, there are many widely used programs designed to estimate the spatial relationship

among populations (e.g., *SPACEMIX* [Bradburd, Ralph, & Coop, 2016]), spatial sub-structuring within populations (e.g., *STRUCTURE* [Pritchard, Stephens, & Donnelly, 2000] and *GENELAND* [Guillot, Mortier, & Estoup, 2005]), and historical migration events among populations (e.g., *EEMS* [Petkova, Novembre, & Stephens, 2016]). A common feature of all these programs is that they use Bayesian algorithms in reconstructing the ancestral status of species populations, which typically follow the island population model (Latter, 1973) that assumes Hardy-Weinberg equilibrium within populations (Saenz-Agudelo, Jones, Thorrold, & Planes, 2009), with less consideration of genetic exchange events among populations. Such Bayesian programs are capable of detecting population genetic patterns from the reconstructed ancestral status of populations, which reflect the results of long-term evolution. However, the programs are not well suited

for application to a single population or geographically continuous populations with high connectivity (Lowe & Allendorf, 2010; Manel, Gaggiotti, & Waples, 2005; Petkova et al., 2016). Another disadvantage of the programs is that most of them are computationally intensive. Therefore, using Bayesian landscape genetic programs to study population genetic patterns and management situations associated with ongoing dispersal over relatively small spatial extents, for example across a city or a nature reserve, is not practical.

To cope with some of these management issues, over the last decade researchers have started to develop non-Bayesian programs. These programs can be classified into two types, one that requires prior knowledge of environmental features and another one that does not:

1. The programs requiring prior knowledge on environmental features (e.g., *CIRCUITSCAPE* [McRae & Shah, 2009], *RESISTANCEGA* [Peterman, 2014] and *SDMTOOLBOX* [Brown, 2014]) normally ask users to input raster layers indicating certain landscape classes or other environmental features. It is possible to input multiple raster layers into some of these programs, which could then be used to define continuous resistance surfaces based on expert decision or an optimization process (Spear, Balkenhol, Fortin, McRae, & Scribner, 2010). This can help prevent subtle fine-scale spatial variation in resistance values being overlooked. The programs generally assume that different landscape classes, or landscape classes combined with other environmental features (Spear et al., 2010), are correlated with resistance and generally calculate the correlation coefficients using genetic algorithms derived from circuit theory (McRae, 2006; McRae & Beier, 2007). These programs can be quite informative for management by providing resistance values over the entire targeted area. However, the accuracy of the programs can be highly dependent on the resolution and the comprehensiveness of the collected environmental data. In addition, assigning fixed resistance values to a particular environmental feature, or combination of environmental features, may overlook the contribution of nonenvironmental factors to dispersal (for example genetic drift), especially when environmental features only explain a minor proportion of spatial genetic divergence (Wang, Glor, & Losos, 2013).
2. The non-Bayesian programs that do not require prior knowledge on environmental features simply map genetic patterns across the study area. Although intuitive, there are only a few such programs available and all of them were published very recently. *Un-PC* (House & Hahn, 2018) is an R package that projects principal components analysis (PCA)-based genetic distances of pairs of populations (the “*un-PC*” values) as ellipses to highlight areas of extreme genetic differentiation and similarity, and therefore areas of high and low resistance. *Un-PC* is model-free in the sense that it does not specify a particular mechanistic model underlying the observed genetic pattern. However, *Un-PC* is designed for mapping spatial genetic patterns among multiple discrete populations because resistance is calculated based on *un-PC* values that are

population-based instead of individual-based. Therefore, it is not suitable for mapping patterns within a population or amongst geographically continuous populations. Another program is *MAPI* (Piry et al., 2016), which works similarly to *Un-PC* and is model-free in the same sense. However, *MAPI* directly projects ellipses representing genetic distances between pairs of individuals, which ignores population-level correlations between genetic distance and environmental features. Moreover, *MAPI* is implemented in the open source database *POSTGRESQL* (Momjian, 2001), which requires relatively complicated database installation and configuration (House & Hahn, 2018). In contrast, a third program, *DResD*, is presented in the form of an R script and calculates resistance using population-level information (Keis et al., 2013). Specifically, *DResD* first calculates the general trend of isolation by distance (IBD) at a population level by fitting an asymptotic curve to data on genetic and geographical distance for all sampled pairs of individuals, and then calculates the IBD residuals of each pair of individuals (Keis et al., 2013). Afterwards, *DResD* computes the resistance in each grid cell as the weighted average of all IBD residuals, with the weights being inversely proportional to the geographical distance between the centre of the cell and the midpoints of lines connecting the corresponding sample pairs over the area considered. This method is thus different from directly projecting the IBD residuals for each sample pair, and therefore strongly departs from *MAPI*. However, in *DResD*, the method of weighting IBD residuals could introduce inaccuracies because only the midpoints of the lines connecting sample pairs are used in calculating resistance, which results in loss of spatial information from all other points in the study area that intersect the connecting lines between sample pairs. Moreover, this method means that each grid cell will receive weighted IBD residuals corresponding to all sample pairs, even though most sample pairs may not be relevant to the focal cell. For example, if the area in a grid cell contains the midpoint of a line with a strongly positive residual, then this could unduly influence the resistance value of the area in a neighbouring grid cell with midpoints that have negative residuals. A minimum distance threshold could be set to avoid this problem, but it is unclear how to objectively set this threshold. In particular, the method of calculating resistance in *DResD* may limit its ability to map resistance over an area with a mosaic pattern.

Inspired by these pioneer non-Bayesian programs and with the motivation of overcoming the limitations identified, we have developed a new individual-based, spatially explicit program for mapping resistance to ongoing dispersal within a single population or amongst geographically continuous populations at relatively small spatiotemporal scales—*ResDisMapper*. More specifically, by “scale” here, we mean “extent” and not “resolution.” *ResDisMapper* is a non-Bayesian program that is implemented as an R package. It calculates resistance for a focal cell as the average of the IBD residuals corresponding to those lines that connect sample pairs and intersect the focal cell. This enables *ResDisMapper* to be used to study population genetic patterns and management

situations associated with ongoing dispersal over relatively small spatiotemporal scales, in contrast to Bayesian programs. In addition, *ResDisMapper* is intuitive, not computationally intensive and belongs to the class of non-Bayesian programs that require no prior knowledge of environmental features. Within this class of non-Bayesian programs, *ResDisMapper* is similar to *DResD* in that they both calculate IBD residuals in the same way, but *ResDisMapper* differs fundamentally from *DResD* by using a novel method to calculate resistance using the IBD residuals, which overcomes the key limitations of *DResD* identified above.

2 | MATERIALS AND METHODS

2.1 | Description of the R package

Our program is called *ResDisMapper*, short for Resistance to Dispersal Mapper. *ResDisMapper* is compiled as an R package allowing for the calculation and visualization of resistance to dispersal. The principle behind *ResDisMapper* is to first calculate the IBD residual for each sample pair of individuals, which is the deviation from the general IBD trend, and then spatially map resistance calculated using the IBD residuals, to see where extreme residuals are accumulated. Positive IBD residuals represent greater genetic distances than the general IBD trend and accumulate in cells which have a relatively high resistance to dispersal, and vice versa for negative IBD residuals. Because the IBD residuals are defined relative to a general IBD trend at the population level, resistance as calculated in *ResDisMapper* is not an absolute value but rather a relative value. For example, in a biological invasion scenario, areas with negative resistance values can be interpreted as areas with human-facilitated dispersal of an invasive species, whereas in a habitat fragmentation scenario, areas with negative resistance values can be interpreted as remaining "corridors" of habitat that have low resistance to dispersal compared with areas cleared of habitat.

ResDisMapper is particularly suited for small spatial scales because the IBD-based approach to calculating resistance should only be applied to a single population or spatially continuous populations that correspond to only one IBD trend. Spatially discrete populations would probably correspond to multiple IBD trends, which would violate the assumption of one IBD trend. In addition, *ResDisMapper* is particularly suited for small temporal scales because the IBD-based approach to calculating resistance assumes that the observed genetic differentiation arises due to geographically limited dispersal, which occurs over short temporal scales at small spatial scales. Thus, the approach is poor at capturing genetic differentiation arising from mutation or historical events over large temporal scales.

The R package comprises four functions corresponding to modelling IBD (*rdm_IBD*), calculating IBD residuals (*rdm_IBD* and *rdm_residual*), mapping and validating resistance (*rdm_resistance*), and visualization (*rdm_mapper*). The R package, example data sets and

user manual are available on Github (<https://github.com/takfung/ResDisMapper>).

2.2 | Description of the workflow

ResDisMapper calculates IBD residuals using individual-based genetic/genotypic differentiation. Running *ResDisMapper* requires genetic and geographical data of samples from a single population or a set of geographically continuous populations which display a genetic pattern that is near-panmictic or that follows a continuous geographical cline, whereby relatedness between samples is largely determined by the physical distance between them. The input data for *ResDisMapper* are two files: a GENEPOP format file for genetic/genotypic information of all sampled individuals and a tab-delimited table for the geographical coordinates of sampling localities. Although designed primarily for single nucleotide polymorphism (SNP) and microsatellite data, *ResDisMapper* can intake data from any genetic markers if they are coded into GENEPOP format through the function provided in the R package *ADEGENET* (Jombart, 2008). *ResDisMapper* allows missing data in the input—missing data are removed during calculation of the IBD residuals. The following are in-depth explanations of the functions in the R package.

The function *rdm_IBD* generates two distance matrices from the input genetic/genotypic data and geographical data, respectively. In generating the genetic distance matrix, *rdm_IBD* adopts the algorithms in the R package *POPPR* (Kamvar, Tabima, & Grünwald, 2014), which provides users with six methods of calculating individual-based genetic distance: relative similarity, Nei's distance, classical Euclidean distance, co-ancestry coefficient, angular distance and absolute genetic distance.

Because *ResDisMapper* focuses on relatively small areas where the curvature of the Earth's surface can be ignored, the geographical distance is calculated simply as the Euclidean distance using the function *dist()* in R.

The two matrices are then used to model the IBD trend for the entire set of sampled individuals. The function *rdm_IBD* provides two ways to model this IBD trend: (a) the linear model and (b) the nonlinear model, where x is geographical distance, y is genetic distance, and a , b and c are constant parameters:

$$y = a + bx \quad (1)$$

$$y = a + b(1 - \exp(-\exp(cx))) \quad (2)$$

More specifically, the parameter a represents the intersect of the IBD trend with the y -axis, the parameter b represents the slope of the IBD trend for the linear model and defines the asymptotic value of y for the nonlinear model, and the parameter c in the non-linear model represents the rate at which the asymptotic value of y is reached as x increases. The values of the three parameters are determined automatically by the function *rdm_IBD*

by minimizing the sum of squared errors between the fitted model and the data points. Afterwards, *rdm_IBD* calculates the IBD residuals, using either Equation 3 for the linear IBD model or Equation 4 for the nonlinear IBD model, where r_i is the residual for the i th pair of sampled individuals and x_i and y_i are the observed geographical and genetic distances for the i th pair of sampled individuals, respectively:

$$r_i = y_i - (a + bx_i) \quad (3)$$

$$r_i = y_i - (a + b(1 - \exp(-\exp(cx_i)))) \quad (4)$$

Finally, *rdm_IBD* creates a scatter-plot of genetic and geographical distances for all pairs of sampled individuals and draws the expected IBD trend through the data space.

The function *rdm_residual* intakes IBD residuals for each pair of sampled individuals (from the output of function *rdm_IBD*) together with their geographical coordinates, and then creates a 3-D graph showing the residuals for each pair of sampled individuals, represented as a line segment over the area considered. In this function, users can specify the geographical distance range over which IBD residuals are considered when calculating resistance. This is important because different spatial scales can give substantially different patterns (Schregel et al., 2018). The geographical distance range can be specified by either (a) using prior knowledge of the typical dispersal range of the species under consideration, or (b) testing different spatial scales and seeing which scale corresponds to that where the genetic correlation between individuals reaches zero (Epperson, 2005). Finally, *rdm_residual* outputs an object of class *SpatialLinesDataFrame*, containing coordinates of the line segments joining each pair of sampled individuals and the corresponding IBD residuals.

The function *rdm_resistance* intakes the object of class *SpatialLinesDataFrame* from the output of *rdm_residual*, projects the line segments onto a user-specified 2-D grid, and calculates the resistance and the associated statistics over the grid. Using the function *rasterize()* in the R package *RASTER* (Hijmans & van Etten, 2014), *rdm_resistance* calculates four statistics for each grid cell: (a) the resistance, (b) the number of intersecting line segments, (c) statistical certainty of the resistance and (d) statistical significance of the resistance. The resistance for a grid cell is the mean of the IBD residual values of all line segments that intersect the cell and have a length within the user-defined geographical distance range. Positive resistance indicates obstruction/deterrence of dispersal through a grid cell due to some geographical property, whereas negative resistance indicates facilitation of dispersal through it. Figure S1 shows a schematic diagram of how resistance values are calculated by *ResDisMapper* and *DResD*.

The statistical certainty of a resistance value in a grid cell represents the certainty of whether the deterrence or facilitation of dispersal through a grid cell is actually taking place, given a set of IBD residuals corresponding to line segments that intersect the cell. This certainty is calculated as the sign of the product of the upper and lower limits of the 95% confidence interval of IBD

residuals for the cell, which accounts for sampling error—if the sign is positive, then the upper and lower limits are of the same sign, indicating probable deterrence or facilitation of dispersal. The upper and lower limits of the 95% confidence interval are calculated using the function *CI* implemented in the R package *RMISC* (Hope, 2013). The statistical significance of the resistance value of a grid cell indicates the degree to which the value differs from those in a null distribution. Specifically, the resistance value for a grid cell is calculated as the average of n IBD residuals, corresponding to n lines intersecting the cell. Analogously, a resistance value from the null distribution for the cell is calculated by (a) randomly sampling (without replacement) n IBD residuals from the set of all IBD residuals corresponding to all lines over the entire area considered, and (b) determining the average of the sampled IBD residuals. The function *rdm_resistance* performs steps (a) and (b) 1,000 times, resulting in 1,000 null values of the resistance values, which form the null distribution. The function then compares the observed resistance value to the null distribution. If the observed resistance of a grid cell is situated above the 95th percentile or below the 5th percentile of the null distribution, then the grid cell is considered as having a high or low resistance that is statistically significant, respectively. There are options within *rdm_resistance* to change the thresholds for determining the statistical certainty and statistical significance of resistance values.

After running *rdm_resistance*, the function will output a data frame showing the summary statistics pertaining to resistance for each grid cell, as described in the previous paragraph. Users can then input the data frame into the function *rdm_mapper* to visualize the resistance map. There is a parameter specifying whether to display all cells (regardless of statistical certainty or not) or only cells with statistical certainty. In addition, there is a parameter specifying whether to draw contour lines delineating grid cells that have resistance values with high statistical significance. A contour line is drawn through adjacent grid cells for which resistance values can be calculated. If a contour line is drawn through a grid cell for a second time, then it forms a loop. However, if a contour line encounters a grid cell with no data (no intersecting line segments) for calculating a resistance value, then the line terminates without forming a loop. There are a few other parameters that users can change to customize the visualization, for example a parameter that specifies the size of the points representing sampling locations.

2.3 | Simulated data set

To demonstrate the utility of *ResDisMapper* and evaluate its performance, we ran *ResDisMapper* with both simulated and empirical data sets. We simulated the genetic dynamics of two species of “unicorns” (abstract species) across a gridded area with two types of landscape, using *SIMADAPT* version 1.8.0 (Rebaudo et al., 2013). In the simulated area, we refer to a grid cell as a “landscape cell,” to differentiate this from a grid cell in the gridded area used by *ResDisMapper* to calculate resistance values. *SIMADAPT* is an

individual-based genetic model for simulating landscape management impacts on populations, and is implemented in *NETLOGO* version 5.1.0 (Wilensky, 1999).

In the simulations, we set up two types of landscape: an unsuitable habitat which we consider to be a barrier to dispersal (with parameter values resource = 1 and barrier = 100) and a suitable habitat (with parameter values resource = 10 and barrier = 0). In *SIMADAPT*, the “resource” parameter for a landscape cell is its carrying capacity expressed as the number of individuals, and the “barrier” parameter for a landscape cell specifies the threshold number of individuals in a neighbouring landscape cell for there to be immigration of individuals from that neighbouring cell. By choosing a resource parameter value of 10 for suitable habitat and a barrier parameter value of 100 for unsuitable habitat, we ensure that there was no immigration from suitable to unsuitable habitats. Thus, we consider the unsuitable habitats in the simulations as “absolute” barriers.

For the setup of genetic markers, we used 100 bi-allelic loci, which were subjected to a mutation rate of 10^{-4} mutations per generation. All the genetic markers were set as neutral to avoid selection.

For the setup of the population, we simulated two species of unicorns, one with low per-capita dispersal probability (0.1, the golden unicorn) and the other with high per-capita dispersal probability (0.5, the silver unicorn). The simulation allows individuals in a focal landscape cell to disperse one landscape cell per generation, to an adjacent landscape cell (eight directions) that has a barrier parameter lower than or equal to the number of individuals in the focal landscape cell. In addition, the number of individuals in a landscape cell was subjected to the logistic growth model with a fixed growth rate of 0.5 per time-step.

We designed two scenarios to simulate both biological invasion and habitat fragmentation. For the biological invasion scenario, we set the initial configuration as 10 individuals in the landscape cell in the bottom-left corner of the grid, while for the habitat fragmentation scenario, we set the initial configuration as 10 individuals in every landscape cell. In each scenario, we had two landscape arrangements, one with a single barrier and the other with two barriers. We used two arrangements in order to test the ability of our program to handle landscapes of varying complexity. The barriers were designed to not separate the entire area into completely isolated areas, to ensure that the individuals across the landscape consist of a single population.

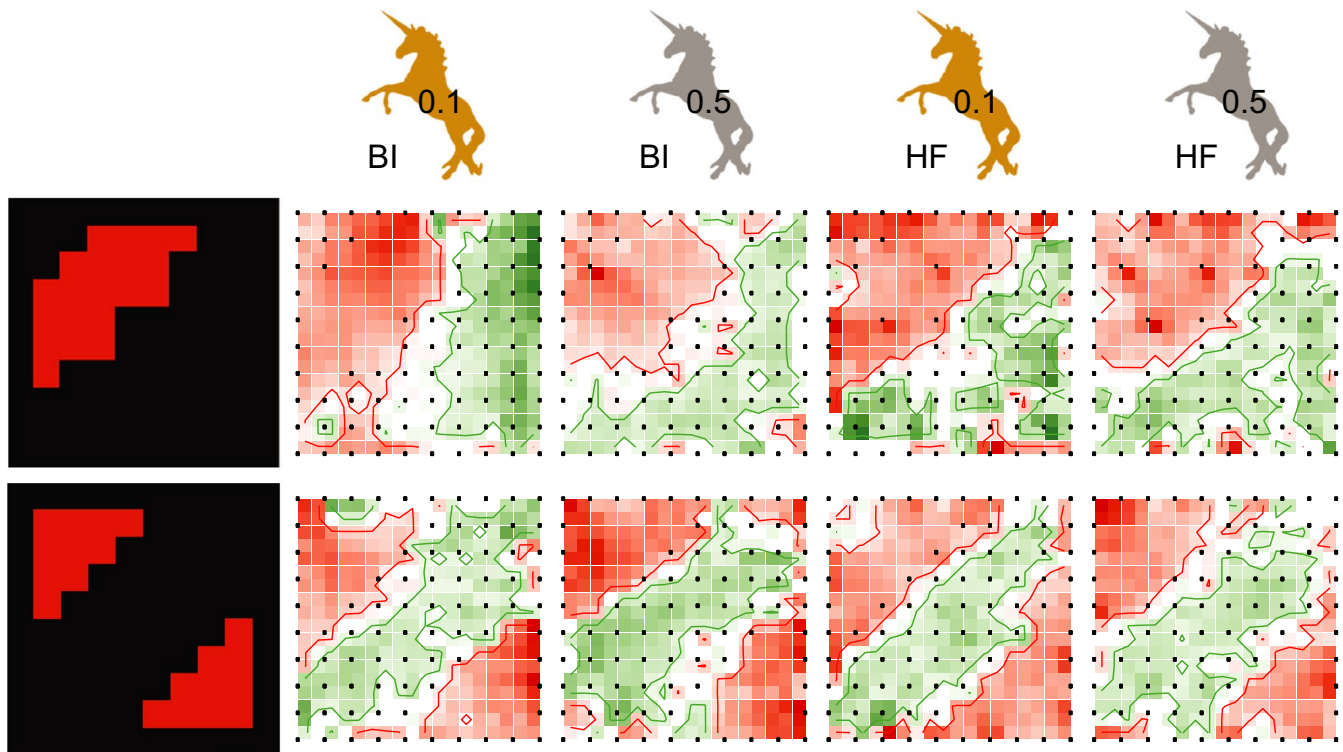


FIGURE 1 *ResDisMapper* results for simulated data sets corresponding to two species of unicorns over areas with absolute barrier(s), after 60 generations. The simulated areas (black cells being suitable habitat and red cells being barriers) are shown in the left-most column. In each row, the simulated area is followed by *ResDisMapper* results for four simulated scenarios (red is high resistance; green is low resistance; red and green contour lines delineate areas with statistically significant high or low resistance, respectively; cells with no statistical certainty are not displayed; and black circles are sampling locations). The number on each unicorn indicates the dispersal probability. In addition, “BI” next to a unicorn indicates a biological invasion scenario, whereas “HF” indicates a habitat fragmentation scenario. Scale bars for resistance values are omitted as each map is for an independent data set, such that quantitative comparison of resistance values among graphs is not meaningful [Colour figure can be viewed at wileyonlinelibrary.com]

All simulations were run on a 10×10 grid. Each simulation lasted 200 generations, sampling every 20 generations. In each sampling event, we randomly sampled three individuals (subject to availability) from each landscape cell. The genotypic data of 100 loci for the samples were then exported for subsequent analyses.

For all the simulated data sets, we used the co-ancestry coefficient method (Reynolds, Weir, & Cockerham, 1983) to calculate the genetic distance under the nonlinear model for IBD modelling. We also tested the five other methods for calculating genetic distance (as per the *R* package *POPPR*), and found that they resulted in similar resistance maps to those using the co-ancestry coefficient method. Thus, we only present results using the co-ancestry coefficient method. When calculating IBD residuals and resistances, we included all pairwise comparisons between sampled individuals. To illustrate the distribution of resistance over the simulated area, we mapped the resistance onto an 18×18 grid using *ResDisMapper*. We used an 18×18 grid to calculate and visualize resistance because of the following chain of reasoning. *ResDisMapper* visualizes resistance over an area that is delimited by the coordinates of the individuals. Because each simulated individual is placed at the centre of the landscape cell that it is in, the portion of the landscape considered by *ResDisMapper* only covers the interior of the full 10×10 grid of landscape cells, which excludes a "border" with a width equal to half a landscape cell (Figure 1). This suggests that resistance should be calculated and visualized using a 9×9 grid. However, this would result in one grid cell containing simulated individuals from more than one location (set of coordinates), that is from more than one of the landscape cells (Figure 1). To eliminate this incompatibility, we used an 18×18 grid for calculation and visualization of resistance (Figure 1).

The geographical coordinates and genetic data for the sampled individuals in the *SIMADAPT* simulations can be downloaded from Github (https://github.com/takfung/ResDisMapper/tree/master/Example_datasets). The files containing the data are labelled according to the scenario simulated, with the type of landscape area (single or double barrier), biological scenario (biological invasion or habitat fragmentation), unicorn species (golden or silver) and number of generations (60 or 200) given in each label. In addition, the files specifying the two types of landscape area (with a single or double barrier) can be downloaded from Github (https://github.com/takfung/ResDisMapper/tree/master/Example_datasets); these files are used in the program *SIMADAPT*. There are three files for each type of landscape area: (a) a "barrier file" that gives the coordinates of each landscape cell together with corresponding values of the barrier parameter; (b) a "resource file" that gives the coordinates of each landscape cell together with corresponding values of the resource parameter; and (c) a "type file" that gives the coordinates of each landscape cell together with a number for each cell indicating whether it is a barrier or not (the latter has a barrier parameter value of 0).

2.4 | Empirical data sets

We chose empirical data sets from two recently published studies to demonstrate the use of *ResDisMapper* in the two scenarios of biological

invasion and habitat fragmentation. Both studies fit the criteria of small temporal (<200 generations) and spatial scales (<1,000 km²). For the biological invasion scenario, we chose a rock pigeon (*Columba livia*) study in Singapore (Tang, Low, Lim, Gwee, & Rheindt, 2018). As stated in their paper, the rock pigeons form a single population whose introduction dates back to 12.5 generations (~15–85 years) ago (Tang et al., 2018). For the habitat fragmentation scenario, we chose the golden-crowned sifaka (*Propithecus tattersalli*) study in the Daraina area in northern Madagascar (Quéméré, Crouau-Roy, Rabarivola, Louis Jr, & Chikhi, 2010). As stated in a follow-up paper (Salmona, Heller, Quéméré, & Chikhi, 2017), the golden-crowned sifaka was near-panmictic throughout the region and then shrank to fragmented habitats ~80 generations (~300–1,500 years) ago. We downloaded the genetic and geographical data for both studies from online data repositories and converted them to the GENEPOP format and tab-delimited table format, respectively.

For both empirical data sets, we used the co-ancestry coefficient method (Reynolds et al., 1983) to calculate the genetic distance under the nonlinear model for IBD modelling. The five other methods for calculating genetic distance (as per the *R* package *POPPR*) produced similar resistance maps to those using the co-ancestry coefficient method. Thus, we only present results using the co-ancestry coefficient method. For each data set, we used results from a spatial autocorrelation analysis to determine the geographical distance at which the genetic correlation between individuals reaches zero, and set the maximum geographical distance in *ResDisMapper* to this distance value when calculating resistance. More specifically, this maximum geographical distance determines which sample pairs to include for calculation of resistance values based on IBD residuals corresponding to sample pairs. In addition, we examined how the resistance values changed as the maximum geographical distance varied below and above the value at which the genetic correlation reaches zero, to assess the sensitivity of our results across different spatial scales. In total, for the pigeon data set, we ran six independent analyses using sample pairs within 5, 10, 15, 20, 25 and 30 km. For each analysis, we projected the distribution of the resistance onto a 50×25 grid, given that the dimension of Singapore Island is around 50×25 km. We also ran analyses using sample pairs within distances >30 km, but these gave similar results to those from using a distance of 30 km; hence, these results are not presented. For the sifaka data set, we ran nine independent analyses using sample pairs within 5, 10, 15, 20, 25, 30, 35, 40 and 45 km. For each analysis, we projected the distribution of the resistance onto a 40×45 grid, given that the dimension of the studied area is around 40×45 km. We also ran analyses using sample pairs within distances greater than 45 km, but these gave similar results to when using a distance of 45 km; hence, these results are not presented.

2.5 | Comparison with other methods

To evaluate the performance of *ResDisMapper*, we compared the results of *ResDisMapper* to those from two other programs: one non-Bayesian program, *DRESD* (Keis et al., 2013), and one Bayesian

program, *EEMS* (Petkova et al., 2016). We ran all three programs on two sets of simulated data. One data set was simulated on an area with absolute barriers, whereas the other data set was simulated on an area with permeable barriers that provide a continuous gradient of resistant values (Shirk, Landguth, & Cushman, 2018). The first data set was simulated using *SIMADAPT*, as described in section 2.3. The second data set was randomly chosen from 450 resistance surfaces that have continuous resistance values, as provided in Shirk et al. (2018) (we randomly chose the data set named *set3_r5_model2*). Using this chosen data set, we ran all three programs with the simulated genetic data extracted at generation 5 and generation 100, to calculate resistance over a 256×256 grid.

As all three programs require the input of pairwise genetic distance matrices, we used the co-ancestry coefficient method as implemented in *POPPR* to calculate the genetic distance matrices. In this manner, all three programs are run with the same genetic distance matrices to avoid differences introduced by using different methods of calculating genetic distance. For *DResD* and *ResDisMapper*, we used the nonlinear model to fit the IBD trend that was used to calculate IBD residuals.

For *DResD*, we adjusted some of the default parameters according to the simulated spatial scale, but otherwise used the default parameters. For *EEMS*, we again adjusted some of the default parameters according to the simulated spatial scale and number of loci, but otherwise used the default parameters. We also monitored the Markov chain Monte Carlo (MCMC) logs visually to ensure convergence of the posterior probability distribution. For the simulated data set with absolute barriers, we ran 10,000,000 MCMC iterations as a burn-in period and then a further 10,000,000 iterations. For the simulated data set with permeable barriers, we ran 20,000,000 MCMC iterations as a burn-in period and then a further 20,000,000 iterations, reflecting more iterations required for convergence.

We used confusion matrices to evaluate the performance of *ResDisMapper*, *DResD* and *EEMS* when applied to the simulated data sets corresponding to the simulated areas with absolute barriers. To construct the confusion matrix for each program, we first determined the number of “positive” cells in the simulated area, which are those with high resistance values that have statistical significance and certainty (*ResDisMapper*), statistical significance and power (*DResD*), or statistical significance (*EEMS*). The remaining cells are classified as “negative”. We then determined the proportion of positive cells that are true positives (i.e., that coincide with the absolute barriers). Similarly, we also determined the proportion of negative cells that are true negatives (i.e., that do not coincide with absolute barriers). In the *SIMADAPT* simulations used to generate the simulated data sets, individuals in a landscape cell can only move to an adjacent landscape cell in one generation, such that in the gridded area used for calculating resistance, nonbarrier cells adjacent to barrier cells are most likely to be classified erroneously as positive cells. Thus, we also calculated confusion matrices whereby a positive nonbarrier cell adjacent to a barrier cell is not considered as a false positive. After calculating the confusion matrices for each of the three programs, we used the entries in the confusion matrices to calculate

metrics evaluating how well the programs performed in classifying cells as barriers and nonbarriers. The metrics we calculated were the kappa statistic (Cohen, 1968), the F1 score (Sasaki, 2007), Youden's J (Youden, 1950) and Matthews correlation coefficient (Matthews, 1975).

To evaluate the performance of a program when applied to a simulated data set corresponding to a simulated area with permeable barriers, we used *R* to calculate the correlation between the simulated resistance values in the grid cells and the corresponding resistance values calculated by the program.

3 | RESULTS

3.1 | Testing *ResDisMapper* using simulated data sets

Results from the data sets simulated using *SIMADAPT* indicate that *ResDisMapper* can conclusively detect barrier(s) by mapping high resistance with statistical certainty and significance (Figure 1). Increasing the complexity of landscape features (from one barrier to two barriers) does not substantially reduce the accuracy (Figure 1 and Figure S2). *ResDisMapper* is capable of mapping resistance to dispersal with high accuracy for both biological invasion and habitat fragmentation scenarios (Figure 1 and Figure S2). *ResDisMapper* also provides consistency of mapping resistance to dispersal for groups of organisms with different dispersal probabilities, as demonstrated by the results of resistance mapping on the two species of unicorns being relatively consistent under equal landscape features. Moreover, within the time range we examined for both biological invasion and habitat fragmentation scenarios, the results of mapping resistance are consistent across different numbers of generations (Figure 1, Figures S2 and S3).

3.2 | Applying *ResDisMapper* to empirical data sets

Our *ResDisMapper* results on the pigeons in Singapore indicate high resistance to dispersal in central and western Singapore, which mainly comprise nonfavourable habitats for the rock pigeons such as dense trees and industrial zones. Compared to the mapping of resistance to dispersal in the original study (Tang et al., 2018) using *DResD*, the resistance mapping from *ResDisMapper* is more congruent with the landscape patterns in Singapore (Figure 2 and Figure S4). Congruence between mapped resistance and landscape pattern is found regardless of whether resistance was calculated using sample pairs of individuals within 5, 10, 15, 20, 25 or 30 km (Figure S4). However, as more sample pairs are added to the analysis, the signal of positive resistance, as measured by the statistical significance, becomes weaker (Figure S4). This pattern probably occurs because the inclusion of an increasing number of pairs of individuals that are further apart and not clearly separated by a barrier dampens strong positive signals in resistance calculations. This effect is best

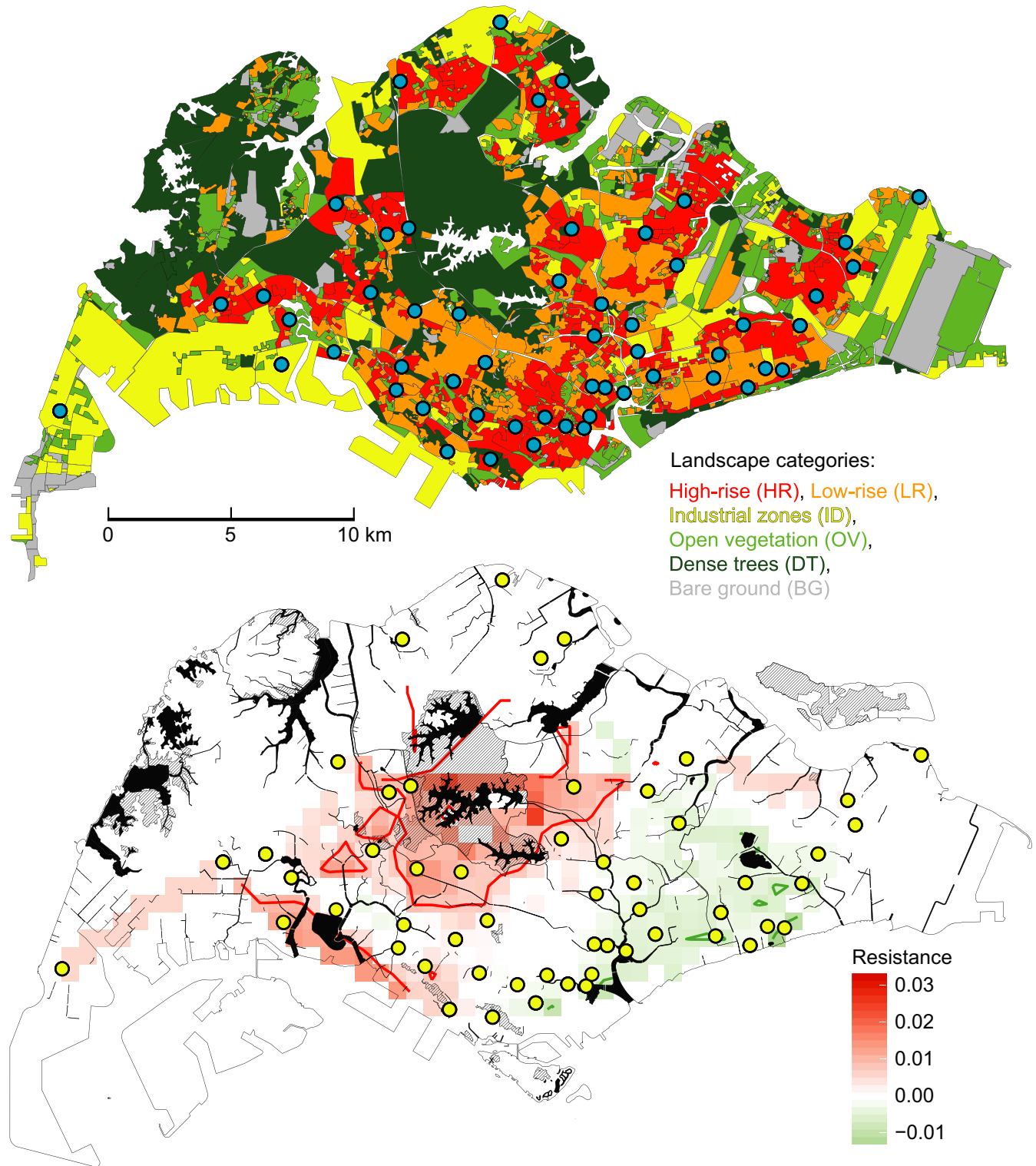


FIGURE 2 *ResDisMapper* results for a biological invasion case study of rock pigeons across Singapore. Top: urban landscape of Singapore. For detailed landscape categorization, please refer to Tang et al. (2018). Blue circles are sampling sites. Bottom: resistance values calculated using *ResDisMapper* with sampled pairs of individuals within 10 km. Red is high resistance; green is low resistance; red and green contour lines delineate areas with statistically significant high or low resistance, respectively; cells with no statistical certainty are not displayed; and yellow circles are sampling sites [Colour figure can be viewed at [wileyonlinelibrary.com](https://onlinelibrary.wiley.com/terms-and-conditions)]

corrected by including only those sampled pairs within the typical range of dispersal. According to a previous spatial autocorrelation analysis, the typical range of dispersal for pigeons in Singapore was

estimated to be within 10 km (Tang et al., 2018). Accordingly, the resistance map derived using only sampled pairs within 10 km should be the most relevant for illustrating the resistance to dispersal of

pigeons in Singapore, and indeed, we found that this map was most congruent with what we expected from the landscape pattern (Figure 2).

For our *ResDisMapper* results on the sifakas in northern Madagascar, we found that regardless of whether resistance was calculated using sampled pairs within 5, 10, 15, 20, 25, 30, 35, 40 or 45 km, the resistance map indicates a consistent pattern of high resistance around the major town, Daraina (Figure 3 and Figure S5). Because the original study (Quéméré et al., 2010) only provided results from a spatial autocorrelation analysis within the range of single forest patches (<5 km), we performed a new analysis using *GenAIE* version 6.5 (Peakall & Smouse, 2006) to calculate the typical range of dispersal of sifakas amongst forest patches. According to the results of this spatial autocorrelation analysis, the typical range of dispersal for sifakas in the area was estimated to be within 15 km (Figure S6). Accordingly, the resistance map derived using only sample pairs within 15 km should be the most relevant for illustrating the resistance to dispersal of sifakas in northern Madagascar, and indeed, we found that this map was most congruent with what we expected from the landscape pattern (Figure 3). In particular, we found that there is high resistance at the interface between the regional major road "National Road 5A" and the river Manankolana (Figure 3). More generally, areas of high resistance to dispersal are either situated along relatively big gaps between patches of dry forest or places of dense human agricultural activity. Also, the *ResDisMapper* results suggest that the forest patches between Daraina and Nosibe may have lost most of their function as a corridor, probably due to relatively intensive human agricultural activity and hunting.

3.3 | Comparison of *ResDisMapper* with other methods

For the 16 simulated scenarios corresponding to the simulated areas with absolute barriers (Table S1; Figure 1, Figures S3, S7 and S8), *ResDisMapper* has a higher percentage of true positives (~18 of all 20 positives) compared to *DResD* (~7) and *EEMS* (~5). *ResDisMapper* also produces a higher percentage of false positives (~20 of all 80 negatives) compared to *DResD* (~6) and *EEMS* (~6). However, we found that ~70% of the false positives *ResDisMapper* produced are adjacent to the actual barriers. If we exclude the false positives adjacent to the actual barriers, then *ResDisMapper* produces a number of false positives (~7) that is on the same order of magnitude compared with *DResD* (~2) and *EEMS* (~3).

ResDisMapper also has the best overall performance for the 16 simulated scenarios when considering the four metrics based on the confusion matrices (kappa, F1 score, Youden's J and Matthews correlation coefficient), regardless of whether we include or exclude false positives adjacent to actual barriers (Figure S2). When there is a single barrier, *ResDisMapper* and *DResD* perform similarly in detecting the barrier; when there are two barriers, *ResDisMapper* performs better than *DResD* and *EEMS* across all eight scenarios (Figure S2). Moreover, *ResDisMapper* has a relatively stable performance across

all 16 scenarios (Figure 1, Figures S2, S3, S7 and S8). In contrast, for some scenarios, *DResD* and *EEMS* produce irregular patterns of resistance values or resistance values that lack statistical significance (Figures S7 and S8), with some metrics falling to 0 (Figure S2).

For the simulated data set corresponding to the simulated area with permeable barriers (Figure S9), we calculated Pearson's correlation coefficient (r) and Spearman's rank correlation coefficient (ρ) to test the correlation between simulated resistance values and resistance values calculated by the three programs. After five generations, resistance values calculated by all three programs exhibited poor correlations with the simulated resistance values ($r_{ResDisMapper} = .023$, $\rho_{ResDisMapper} = 0.010$; $r_{DResD} = .072$, $\rho_{DResD} = 0.087$; $r_{EEMS} = -.048$, $\rho_{EEMS} = -0.045$). This is probably because the individuals have not accumulated sufficient genetic divergence from a randomized initial status, such that the genetic signal is not strong enough for the programs to detect most of the resistance to dispersal. However, after 100 generations, resistance values calculated using *ResDisMapper* achieved a substantially stronger correlation with the simulated resistance values ($r_{ResDisMapper} = .374$, $\rho_{ResDisMapper} = 0.400$), more so than the correlation for *DResD* ($r_{DResD} = .204$, $\rho_{DResD} = 0.260$) and *EEMS* ($r_{EEMS} = -.022$, $\rho_{EEMS} = -0.026$).

4 | DISCUSSION

According to tests on both simulated and empirical data sets, *ResDisMapper* can detect fine-scale patterns of resistance to ongoing dispersal with high accuracy using individual-based genetic data. Among the three landscape genetic programs that we considered, *EEMS* seems to have performed most poorly in our specific test scenarios. A probable reason is that we set the simulated area to the scale of a single population, where all the individuals are not completely isolated. This arrangement may have resulted in high uncertainty in *EEMS* when computing the ancestral status of individuals, because genetically, all individuals are relatively homogeneous. This lack of pronounced population subdivision probably accounted for the difficulty with which the posterior probability distribution reached convergence during *EEMS* runs, as well as the high incidence of irregularities in *EEMS* resistance maps (Figures S7, S8 and S9). In contrast to *EEMS*, *DResD* and *ResDisMapper* are more capable of handling a population in which all the individuals are not completely isolated, with similar performance on simulated areas with a single absolute barrier (Figure 1, Figures S2, S3, S7 and S8). However, *DResD* calculates the resistance value in a grid cell using the IBD residuals from all sampled pairs of individuals, and this may result in dilution of weak local signals by relatively strong but remote signals. We found signs of this dilution when looking at the performance of *DResD* on simulated areas with two absolute barriers (Figure 1, Figures S3, S7 and S8). In this case, for some scenarios, *DResD* only produced high resistance that was statistically significant at one of the barriers, whereas for other scenarios *DResD* did not produce high resistance that was statistically significant at either of the two barriers.

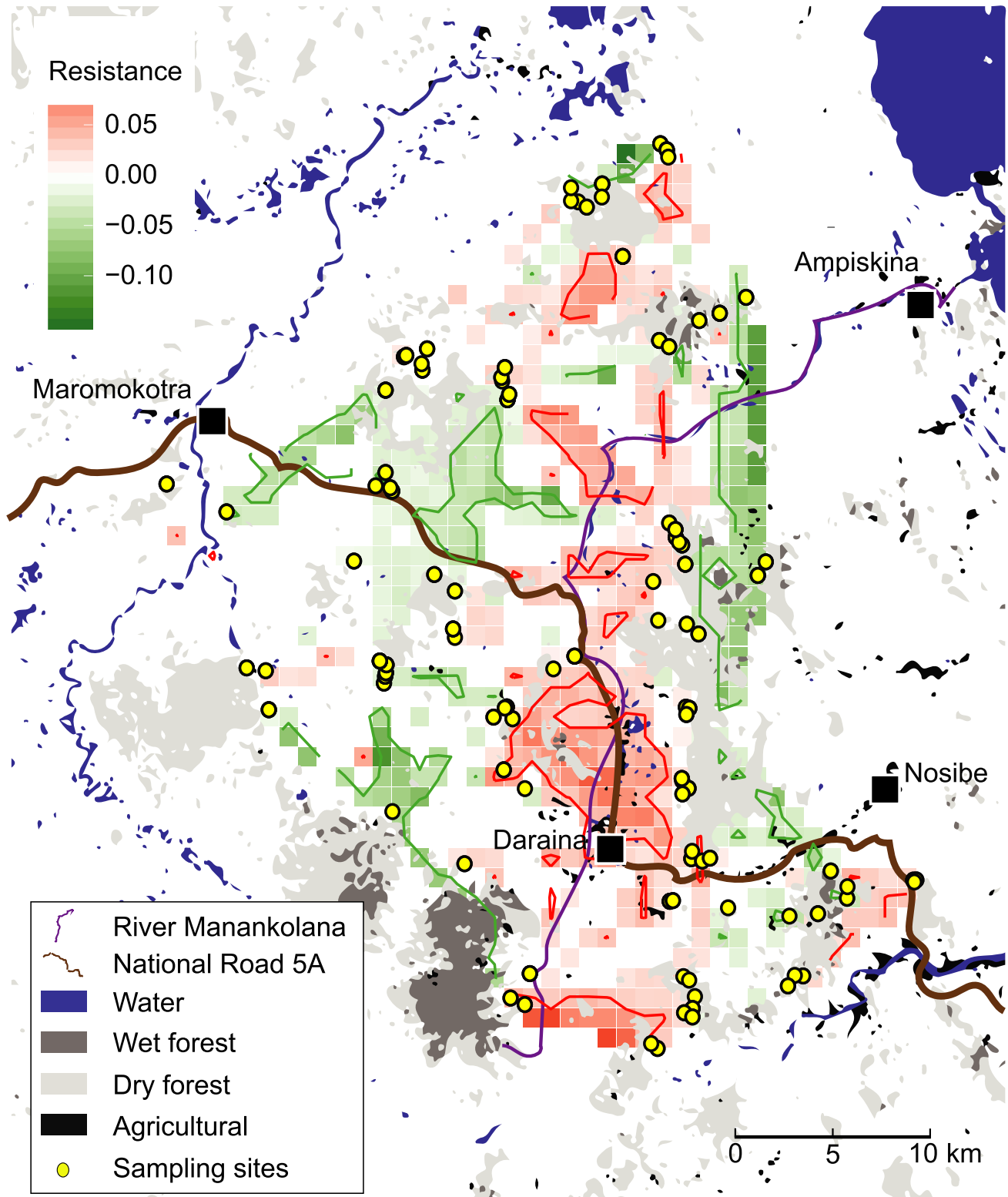


FIGURE 3 *ResDisMapper* results for a habitat fragmentation case study on golden-crowned sifakas in the Daraina area, northern Madagascar. Resistance is calculated using sampled pairs of individuals within 15 km. Red is high resistance; green is low resistance; red and green contour lines delineate areas with statistically significant high or low resistance, respectively; cells with no statistical certainty are not displayed; and yellow circles are sampling sites [Colour figure can be viewed at [wileyonlinelibrary.com](https://onlinelibrary.wiley.com)]

Our tests on the simulated data sets show that *ResDisMapper* can detect fine-scale patterns of resistance to ongoing dispersal accurately, using individual-based genetic data from studies focusing

on a single population or a set of geographically continuous populations. *ResDisMapper* calculates resistance using IBD residuals that are derived from a comparison of genetic and geographical distances

for pairs of individuals with an expected IBD trend. Although this is broadly similar to the way in which some Bayesian programs calculate resistance, our non-Bayesian tool *ResDisMapper* differs by focusing on detecting resistance to ongoing dispersal, without performing simulations to trace back historical migrations. In this manner, *ResDisMapper* aims to resolve real-time management issues at small temporal scales, instead of the ecological and evolutionary history of a species addressed by most Bayesian landscape genetic tools, including *STRUCTURE* (Pritchard et al., 2000), *GENELAND* (Guillot et al., 2005) and *EEMS* (Petkova et al., 2016). For example, for the sifaka data set that we examined, the original study (Quéméré et al., 2010) used *STRUCTURE* to cluster individuals over space according to their ancestral genetic status (i.e., genetic differentiation accumulated via isolation over a very long period of time). The results from *STRUCTURE* showed that there is high genetic differentiation between clusters either side of the Manankolana River (Quéméré et al., 2010; their Figure 2). However, *STRUCTURE* does not emphasize recent dispersal occurring among individuals, which can substantially alter genetic patterns inferred by focusing on ancestral genetic status. Consequently, results from *ResDisMapper* (Figure 3), which focus on more recent causes of resistance to dispersal (such as human settlement, agricultural areas and roads), showed a genetic pattern different to that from *STRUCTURE*. In particular, individuals no longer show a clear genetic separation along the Manankolana River. Instead, there is an area of high resistance around the major town of Daraina as well as the interface between the Manankolana River and the major road, which separate individuals genetically.

Based on our results, we recommend *ResDisMapper* for mapping resistance at small spatiotemporal scales for a single population or geographically continuous populations. Small spatiotemporal scales mean that there is no need to account for selection, mutations or whether a population is expanding or shrinking. In addition, we only recommend using *ResDisMapper* to study populations which do not have signs of major gene flow from immigration. The genotypes that immigrants carry can produce extreme IBD residuals that outweigh the genetic divergence created by resistance to dispersal, thus resulting in erroneous resistance maps.

Because of its simplicity of approach relative to most other existing landscape genetic programs, *ResDisMapper* does have the limitation that it cannot be used to calculate resistance values and associated statistics for grid cells without any intersecting lines that connect the geographical locations of sampled pairs of individuals, or for grid cells with just one intersecting line (because one intersecting line is insufficient for calculating statistical certainty of resistance values). Thus, resistance values for such grid cells can only be calculated by either more comprehensive sampling in and around these cells, or by compromising and reducing the mapping resolution to obtain larger grid cells that contain at least two intersecting lines.

A further consideration is that *ResDisMapper* calculates resistance using IBD residuals that are derived by determining the differences between the genetic distances for a sampled set of

individuals and an expected IBD trend. This expected IBD trend is derived by fitting a linear or saturating function to the pairs of geographical and genetic distances corresponding to the sampled individuals. Hence, the exact shape of the expected IBD trend depends on the sampling scheme and would vary with properties of the sampling scheme, such as sample size. This uncertainty in the expected IBD trend would propagate and introduce uncertainty into the IBD residuals and hence resistance values. We anticipate that the magnitude of this uncertainty would typically be quite small given that the expected IBD trend is typically fitted to many observed pairs of geographical and genetic distances. Nonetheless, to minimize this uncertainty, we encourage the identification of genetic markers that are poorly sampled, which can then be excluded from calculation of the expected IBD trend, IBD residuals and resistance values.

Overall, the utility and accuracy of *ResDisMapper* is fundamentally dependent on the comprehensiveness of sampling, as for all other genetic programs. An alternative method of deriving the expected IBD trend is to use a suitably parameterized mechanistic model. However, such a method would still be affected by sampling uncertainty because the parameters of the mechanistic model need to be estimated using sampled data.

ACKNOWLEDGEMENTS

We thank Ryan Chisholm for valuable advice. We acknowledge a Singapore Ministry of Education Tier 1 grant (WBS R-154-000-691-112) for financial support. Q.T. was funded through a Singapore MSRD grant (WBS R-154-000-A47-281). T.F. was supported by a grant to Ryan Chisholm from the James S. McDonnell Foundation (#220020470).

AUTHOR CONTRIBUTIONS

Q.T. and F.E.R. conceived the idea and designed the project. Q.T. and T.F. wrote the code for the *R* package. Q.T. performed the tests on simulated and empirical data sets. T.F. packaged the code and developed the supporting documentation, with edits by Q.T. Q.T. wrote the user manual for the *R* package, with edits by T.F. Q.T. wrote the paper with F.E.R. and T.F. providing edits.

DATA AVAILABILITY STATEMENTS

The *R* package, user manual and example data sets are available online from: <https://github.com/takfung/ResDisMapper>.

ORCID

Frank E. Rheindt  <https://orcid.org/0000-0001-8946-7085>

REFERENCES

- Bradburd, G. S., Ralph, P. L., & Coop, G. M. (2016). A spatial framework for understanding population structure and admixture. *PLoS Genetics*, 12(1), e1005703. <https://doi.org/10.1371/journal.pgen.1005703>
- Brown, J. L. (2014). SDM toolbox: A python-based GIS toolkit for landscape genetic, biogeographic and species distribution model analyses. *Methods in Ecology and Evolution*, 5(7), 694–700. <https://doi.org/10.1111/2041-210X.12200>

- Cohen, J. (1968). Weighted kappa: Nominal scale agreement provision for scaled disagreement or partial credit. *Psychological Bulletin*, 70(4), 213. <https://doi.org/10.1037/h0026256>
- Dudaniec, R. Y., Rhodes, J. R., Worthington Wilmer, J., Lyons, M., Lee, K. E., McAlpine, C. A., & Carrick, F. N. (2013). Using multilevel models to identify drivers of landscape-genetic structure among management areas. *Molecular Ecology*, 22(14), 3752–3765. <https://doi.org/10.1111/mec.12359>
- Epperson, B. K. (2005). Estimating dispersal from short distance spatial autocorrelation. *Heredity*, 95, 7–15. <https://doi.org/10.1038/sj.hdy.6800680>
- Guillot, G., Mortier, F., & Estoup, A. (2005). GENELAND: A computer package for landscape genetics. *Molecular Ecology Notes*, 5(3), 712–715. <https://doi.org/10.1111/j.1471-8286.2005.01031.x>
- Hijmans, R. J., & van Etten, J. (2014). raster: Geographic data analysis and modeling. R package version, 2(8). <https://CRAN.R-project.org/package=raster>
- Hope, R. M. (2013). Rmisc: Ryan miscellaneous. R Package Version, 1(5). <https://CRAN.R-project.org/package=Rmisc>
- House, G. L., & Hahn, M. W. (2018). Evaluating methods to visualize patterns of genetic differentiation on a landscape. *Molecular Ecology Resources*, 18(3), 448–460. <https://doi.org/10.1111/1755-0998.12747>
- Jombart, T. (2008). adegenet: A R package for the multivariate analysis of genetic markers. *Bioinformatics*, 24(11), 1403–1405. <https://doi.org/10.1093/bioinformatics/btn129>
- Kamvar, Z. N., Tabima, J. F., & Grünwald, N. J. (2014). Poppr: An R package for genetic analysis of populations with clonal, partially clonal, and/or sexual reproduction. *PeerJ*, 2, e281.
- Keis, M., Remm, J., Ho, S. Y. W., Davison, J., Tammeleht, E., Tumanov, I. L., ... Saarma, U. (2013). Complete mitochondrial genomes and a novel spatial genetic method reveal cryptic phylogeographical structure and migration patterns among brown bears in north-western Eurasia. *Journal of Biogeography*, 40(5), 915–927. <https://doi.org/10.1111/jbi.12043>
- Latter, B. D. H. (1973). The island model of population differentiation: A general solution. *Genetics*, 73, 147–157.
- Lowe, W. H., & Allendorf, F. W. (2010). What can genetics tell us about population connectivity? *Molecular Ecology*, 19, 3038–3051. <https://doi.org/10.1111/j.1365-294X.2010.04688.x>
- Manel, S., Gaggiotti, O. E., & Waples, R. S. (2005). Assignment methods: Matching biological questions with appropriate techniques. *Trends in Ecology and Evolution*, 20, 136–142. <https://doi.org/10.1016/j.tree.2004.12.004>
- Manel, S., & Holderegger, R. (2013). Ten years of landscape genetics. *Trends in Ecology and Evolution*, 28(10), 614–621. <https://doi.org/10.1016/j.tree.2013.05.012>
- Manel, S., Schwartz, M. K., Luikart, G., & Taberlet, P. (2003). Landscape genetics: Combining landscape ecology and population genetics. *Trends in Ecology and Evolution*, 18(4), 189–197. [https://doi.org/10.1016/S0169-5347\(03\)00008-9](https://doi.org/10.1016/S0169-5347(03)00008-9)
- Matthews, B. W. (1975). Comparison of the predicted and observed secondary structure of T4 phage lysozyme. *Biochimica Et Biophysica Acta (BBA) - Protein Structure*, 405(2), 442–451. [https://doi.org/10.1016/0005-2795\(75\)90109-9](https://doi.org/10.1016/0005-2795(75)90109-9)
- McRae, B. H. (2006). Isolation by resistance. *Evolution*, 60, 1551–1561. <https://doi.org/10.1111/j.0014-3820.2006.tb00500.x>
- McRae, B. H., & Beier, P. (2007). Circuit theory predicts gene flow in plant and animal populations. *Proceedings of the National Academy of Sciences*, 104, 19885–19890. <https://doi.org/10.1073/pnas.0706568104>
- McRae, B. H., & Shah, V. B. (2009). *Circuitscape user's guide*. Santa Barbara, CA: The University of California.
- Momjian, B. (2001). *PostgreSQL: Introduction and concepts* (Vol. 192). New York, NY: Addison-Wesley.
- Palsbøll, P. J. (1999). Genetic tagging: Contemporary molecular ecology. *Biological Journal of the Linnean Society*, 68, 3–22. <https://doi.org/10.1111/j.1095-8312.1999.tb01155.x>
- Peakall, R. O. D., & Smouse, P. E. (2006). GENALEX 6: Genetic analysis in Excel. Population genetic software for teaching and research. *Molecular Ecology Notes*, 6(1), 288–295.
- Peterman, W. E. (2014). ResistanceGA: An R package for the optimization of resistance surfaces using genetic algorithms. *Methods in Ecology and Evolution*, 9, 1638–1647.
- Petkova, D., Novembre, J., & Stephens, M. (2016). Visualizing spatial population structure with estimated effective migration surfaces. *Nature Genetics*, 48(1), 94. <https://doi.org/10.1038/ng.3464>
- Piry, S., Chapuis, M. P., Gauffre, B., Papaïx, J., Cruaud, A., & Berthier, K. (2016). Mapping Averaged Pairwise Information (MAPI): A new exploratory tool to uncover spatial structure. *Methods in Ecology and Evolution*, 7(12), 1463–1475. <https://doi.org/10.1111/2041-210X.12616>
- Pritchard, J. K., Stephens, M., & Donnelly, P. (2000). Inference of population structure using multilocus genotype data. *Genetics*, 155(2), 945–959.
- Quéméré, E., Crouau-Roy, B., Rabarivola, C., Louis Jr, E. E., & Chikhi, L. (2010). Landscape genetics of an endangered lemur (*Propithecus tattersalli*) within its entire fragmented range. *Molecular Ecology*, 19(8), 1606–1621.
- Rebaudo, F., Rouzic, A., Dupas, S., Silvain, J. F., Harry, M., & Dangles, O. (2013). SimAdapt: An individual-based genetic model for simulating landscape management impacts on populations. *Methods in Ecology and Evolution*, 4(6), 595–600. <https://doi.org/10.1111/2041-210X.12041>
- Reynolds, J. B., Weir, B. S., & Cockerham, C. C. (1983). Estimation of the coancestry coefficient: Basis for a short-term genetic distance. *Genetics*, 105, 767–779.
- Richardson, J. L., Brady, S. P., Wang, I. J., & Spear, S. F. (2016). Navigating the pitfalls and promise of landscape genetics. *Molecular Ecology*, 25(4), 849–863. <https://doi.org/10.1111/mec.13527>
- Saenz-Agudelo, P., Jones, G. P., Thorrold, S. R., & Planes, S. (2009). Estimating connectivity in marine populations: An empirical evaluation of assignment tests and parentage analysis under different gene flow scenarios. *Molecular Ecology*, 18, 1765–1776. <https://doi.org/10.1111/j.1365-294X.2009.04109.x>
- Salmona, J., Heller, R., Quéméré, E., & Chikhi, L. (2017). Climate change and human colonization triggered habitat loss and fragmentation in Madagascar. *Molecular Ecology*, 26(19), 5203–5222. <https://doi.org/10.1111/mec.14173>
- Sasaki, Y. (2007). *The truth of the F-measure*. *Teach Tutor mater*, 1(5), 1–5.
- Schregel, J., Remm, J., Eiken, H. G., Swenson, J. E., Saarma, U., & Hagen, S. B. (2018). Multi-level patterns in population genetics: Variogram series detects a hidden isolation-by-distance-dominated structure of Scandinavian brown bears *Ursus arctos*. *Methods in Ecology and Evolution*, 9(5), 1324–1334.
- Shirk, A. J., Landguth, E. L., & Cushman, S. A. (2018). A comparison of regression methods for model selection in individual-based landscape genetic analysis. *Molecular Ecology Resources*, 18(1), 55–67. <https://doi.org/10.1111/1755-0998.12709>
- Spear, S. F., Balkenhol, N., Fortin, M. J., McRae, B. H., & Scribner, K. I. M. (2010). Use of resistance surfaces for landscape genetic studies: Considerations for parameterization and analysis. *Molecular Ecology*, 19(17), 3576–3591. <https://doi.org/10.1111/j.1365-294X.2010.04657.x>
- Storfer, A., Murphy, M. A., Spear, S. F., Holderegger, R., & Waits, L. P. (2010). Landscape genetics: Where are we now? *Molecular Ecology*, 19(17), 3496–3514. <https://doi.org/10.1111/j.1365-294X.2010.04691.x>
- Storfer, A., Patton, A., & Fraik, A. K. (2018). Navigating the interface between landscape genetics and landscape genomics. *Frontiers in Genetics*, 9, 68. <https://doi.org/10.3389/fgene.2018.00068>

- Tang, Q., Low, G. W., Lim, J. Y., Gwee, C. Y., & Rheindt, F. E. (2018). Human activities and landscape features interact to closely define the distribution and dispersal of an urban commensal. *Evolutionary Applications*, 11(9), 1598–1608. <https://doi.org/10.1111/eva.12650>
- Wang, I. J., Glor, R. E., & Losos, J. B. (2013). Quantifying the roles of ecology and geography in spatial genetic divergence. *Ecology Letters*, 16(2), 175–182. <https://doi.org/10.1111/ele.12025>
- Wilensky, U. (1999). *NetLogo*. Center for connected learning and computer-based modeling. Evanston, IL: Northwestern University.
- Youden, W. J. (1950). Index for rating diagnostic tests. *Cancer*, 3(1), 32–35. [https://doi.org/10.1002/1097-0142\(1950\)3:1<32:AID-CNCR2820030106>3.0.CO;2-3](https://doi.org/10.1002/1097-0142(1950)3:1<32:AID-CNCR2820030106>3.0.CO;2-3)

SUPPORTING INFORMATION

Additional supporting information may be found online in the Supporting Information section.

How to cite this article: Tang Q, Fung T, Rheindt FE. *ResDisMapper*: An R package for fine-scale mapping of resistance to dispersal. *Mol Ecol Resour*. 2020;20:819–831. <https://doi.org/10.1111/1755-0998.13127>